CSCE Annual Conference

Growing with youth – Croître avec les jeunes

Laval (Greater Montreal)

June 12 - 15, 2019

PERFORMANCE-BASED DESIGN OF RC BEAMS EXPOSED TO NATURAL FIRE: A CASE STUDY

Kuehnen, R.T.[1,3], Youssef, M.A.[1], El-Fitiany, S.[1,2]

[1] Western University, Department of Civil and Environmental Engineering, London, Canada

[2] Alexandria University, Department of Civil Engineering, Alexandria, Egypt

[3] rkuehnen@uwo.ca

Abstract: In North America, the current practice for structural fire safety involves the implementation of prescriptive methods, requiring compliance with passive fire-resistance barriers and active suppression systems. Although this approach has been largely successful in delaying the propagation of fire, which allows for the safe evacuation of occupants, it provides limited knowledge about expected structural behavior during fire. To ensure structural integrity, the North American industry is moving towards performance-based structural fire design, focusing on structural elements that can achieve specific performance objectives during fire exposure. Buildings can thus be designed with greater flexibility, reduced construction costs, and improved occupancy safety. Given the intrinsic fire-resistant properties of concrete, performance-based design is particularly powerful in the case of reinforced concrete (RC) structures. In this paper, a case study is presented demonstrating a simplified approach to undertake performance-based flexural fire design of RC beams. The case study highlights the three main steps in the design process: (i) determination of the natural fire severity, (ii) calculation of element internal temperatures, and (iii) sectional flexure analysis. In each part, the process is performed using simplified analysis methods, which are validated against results obtained using experimental tests and finite element simulations. Using the approach, engineers can calculate the moment capacity of RC beams to withstand natural fire events.

1 INTRODUCTION

Fire exposure represents one of the most severe loading scenarios for reinforced concrete (RC) buildings. The extreme variability of fire events, in their formation and influence on structural elements, is of major concern to designers. Current practices for fire safety in Canada are outlined by the prescriptive methods in the National Building Code of Canada (NBC, 2015) and the National Fire Code of Canada (NFC, 2015). The prescriptions of these codes are largely based on historic experience, focusing on preventing the spread of fires to allow for the safe evacuation of building occupants and the application of firefighting activities. The NBC's prescriptive methods however provide no knowledge about expected structural behaviour and provide only temporary fire protection. As buildings become larger and taller, safe evacuation within a reasonable time frame is not always feasible. In September of 2018, the fire and subsequent structural collapse at the National Museum of Brazil resulted in the loss of 92 % of its collection; it could not be evacuated in time (Solly, 2018). Other high-profile structural failures at the Plasco Building in 2017 and Windsor Tower in 2005, all clearly demonstrate the limitation of prescriptive fire safety measures. To ensure structural integrity, the industry is moving towards performance-based design, requiring the specification of performance requirements and developing solutions to meet the requirements based on scientific principles. By engaging in the performance design of structures for fire events, buildings can be designed with greater flexibility, reduced construction cost, and improved occupant safety.

Given the intrinsic fire-resistant properties of concrete, performance-based design is particularly powerful in the case of RC structures. In lieu of expensive experimental work or intensive computational analysis, building codes and designers are in need of simplified methods to assess RC members exposed to realistic fire events. In this paper, a case study is presented demonstrating a simplified approach to undertake performance-based flexural fire design of RC beams constructed using normal strength concrete (NSC). The case study highlights the three main steps in the design process: (i) determination of the natural fire severity, (ii) calculation of element internal temperatures, and (iii) sectional flexure analysis. The final result of the analysis is the calculation of sagging and hogging capacities for a RC section undergoing fire exposure (M_{rT}). Application of the simplified process is performed on a section previously tested by Ellingwood and Lin (1991). The simplified analysis is validated with results from the experimental testing and ABAQUS finite element (FE) software. Using the proposed simplified approach, designers will be capable of quickly determining the flexural capacity of RC beams during natural fire events.

2 STRUCTURAL FIRE DESIGN METHODOLOGY

This section presents the methodology for the simplified analysis of RC beams during a natural fire event. The methodology proceeds in three sequential steps. Firstly, the severity of the fire event is determined by developing a natural temperature-time curve for a given compartment. A time equivalent method is then used to find an equivalent standard fire to represent the severity of the natural fire for a RC beam. Secondly, using a simple thermal model presented by Wickström (1986) and the equivalent standard fire from the previous step, the two-dimensional thermal gradients that develop within a RC section are determined. Lastly, flexural analysis is preformed to satisfy concrete equilibrium for both sagging and hogging conditions. Models presented by Youssef and Moftah (2007) are referenced to account for the influence of fire-induced strains and material degradation required for the flexural analysis. The resulting sagging and hogging moment capacities are presented for the fire exposed beam.

2.1 Severity of the Fire Event

Severity of a fire event is best represented by a temperature-time curve, which records a fire's temperature rise with time. The Eurocode provides a simple and well-documented approach to calculate a natural temperature-time curve based on a variety of compartment specific parameters (EN 1991-1-2, 2002). For smaller compartments, the Eurocode approach provides a reasonable and simple representation of fire severity (Buchanan, 2001). When considering larger floor areas, more numerous openings, or increased fuel loads; it is necessary to evaluate the effects of travelling fires (Dai et al., 2017).

In view of the fact that natural temperature-time curves are compartment specific, a time equivalent (t_e) is used to relate the natural fire to the industry standard fire. By defining an equivalent standard fire duration, the wealth of experimental testing and material models derived using the standard fire, can be applied to a specific compartment. For RC beams, time equivalency can be determined based on the internal temperatures that develop within a section during fire exposure. To simplify analysis, the two-dimensional thermal gradients can be represented by a one-dimensional average internal temperature profile (AITP). The AITP is found by dividing a section into a two-way mesh and conducting a heat transfer analysis to record the maximum temperature at each location during fire exposure. The meshed units are subsequently grouped into horizontal layers and the average temperature of each layer is calculated. The resulting AITP represents the maximum temperature experienced by each layer throughout the fire event. Suitability of AITPs in the performance-based design of RC beams resisting uniaxial bending has been proven by El-Fitiany and Youssef (2009). The AITP t_e is conservatively proposed as the shortest duration standard fire that produces equal or larger average temperatures at every layer along the height of the section as compared to the natural fire (Kuehnen, 2019). Although there are many time equivalent methods, the AITP method is tailored specifically for RC beams. Additionally, it is the only method to account for section dimensions. Eq. 1 displays the general equations for the AITP t_e and the size adjustment factor (ψ_{size}) for application with the ISO standard fire (ISO 834, 2014); where T_{max} is the maximum fire temperature (°C), t_{tmax} is the corresponding time (min), t_{final} is the overall duration of the fire (min), h_c is the height of the beam (mm), and b_c is the width (mm). Coefficients are presented in Table 1. Eqn. 1a is only valid for sections of 250 x 500 mm; for sections of larger of smaller dimensions the ψ_{size} must be applied.

[1a] $$t_e = \mathrm{A} + Bt_{max} + Ct_{final} + DT_{max} + Et_{max}^2 + Ft_{final}^2 + GT_{max}^2 + Ht_{max}t_{final} + It_{max}T_{max} + Jt_{final}T_{max}$$

[1b] $$\psi_{size} = \begin{cases} 1.0 \; for \begin{cases} b_c < 300\; mm \\ T_{max} > 1150℃ \\ t_e > 180 \min \end{cases} \\ \\ A + Bt_{max} + Ct_{final} + DT_{max} + \; b_c\left(E + Ft_{max} + Gt_{final} + HT_{max}\right) \; \geq 1.0 \end{cases}$$

Table 1. Coefficients for t_e and ψ_{size} (Eq. 1)

		t_e (Eq. 1a)				ψ_{size} (Eq. 1b)
Valid Range	b_c (mm)	*250*				*200 – 800*
	h_c (mm)	*500*				*300 – 800*
	t_{max} (min)	*15 - 115*				*15 – 115*
	t_{final} (min)	*20 - 240*				*20 – 240*
	T_{max} (°C)	*350 - 750*	*750 - 950*	*950 - 1100*	*1100 - 1200*	*350 – 1200*
Coefficients	A	8.685	2.370	566.30	4404.0	0.819
	B	-0.0829	-0.0893	-0.465	-5.745	3.78×10^{-4}
	C	0.0324	0.0446	1.188	1.039	-2.23×10^{-4}
	D	-0.0428	-0.0186	-1.332	-8.177	1.82×10^{-4}
	E	-4.74×10^{-4}	-9.42×10^{-4}	-20.00×10^{-4}	-80.87×10^{-4}	1.037
	F	-4.16×10^{-4}	-7.39×10^{-4}	0.0	2.99×10^{-4}	-27.00×10^{-4}
	G	0.66×10^{-4}	0.35×10^{-4}	7.95×10^{-4}	38.36×10^{-4}	27.15×10^{-4}
	H	1.57×10^{-4}	4.77×10^{-4}	-3.07×10^{-4}	-17.80×10^{-4}	-10.75×10^{-4}
	I	5.33×10^{-4}	5.40×10^{-4}	12.05×10^{-4}	69.36×10^{-4}	---
	J	3.70×10^{-4}	4.71×10^{-4}	-9.00×10^{-4}	-8.40×10^{-4}	---

2.2 RC Internal Thermal Model

The simplest and best documented thermal model is provided by Wickström (1986). Using Eq. 2, the temperature rise (T) can be calculated at any location (x, y) within a concrete beam. It should be noted that this version of the equation is only valid for three-sided heating from the bottom and two sides. Wickström (1986) provides a modified version for four-sided heating.

[2a] $$T = T_f \left[\eta_w\left(\eta_x + \eta_y - 2\eta_x\eta_y\right) + \eta_x\eta_y\right] \geq 20℃$$

[2b] $$\eta_w = 1 - 0.0616\left(\frac{1550}{\sqrt{kc_s\rho}}\, t_e\right)^{-0.88}$$

[2c] $$\eta_x = 0.23ln\left[\left(\frac{k}{c_s\rho a_c}\,\frac{t_e}{x^2}\right) - 1.09\right] \geq 0 + \; 0.23ln\left[\left(\frac{k}{c_s\rho a_c}\,\frac{t_e}{(b-x)^2}\right) - 1.09\right] \geq 0$$

[2d] $$\eta_y = 0.23ln\left[\left(\frac{k}{c_s\rho a_c}\,\frac{t_e}{y^2}\right) - 1.09\right] \geq 0$$

Where T_f is the fire temperature of the compartment (°C) during exposure to the ISO-standard fire at duration t_e (hr), x is the distance of the point under consideration to the closer of the left or right face (mm), and y is the distance from the bottom side (mm). The dimensionless terms η_w, η_x, and η_y are the ratios of the beam's surface temperature to that of the fire temperature, the temperature at interior point x, and the temperature at interior point y, respectively. To account for variable concrete properties: k is the thermal conductivity ($Wm^{-1}K^{-1}$), ρ is the concrete density (kgm^{-3}), c_s is the specific heat of concrete ($Jkg^{-1}K^{-1}$), and a_c is the thermal diffusivity of concrete (m^2s^{-1}).

2.3 Fire-Induced Strains and Material Models

Fire-induced strains consist of three terms: stress-related strain (ε_{fT}), free-thermal strain (ε_{th}), and transient strain (ε_{tr}) (Youssef and Moftah, 2007). Concrete's stress-related strain is a function of the applied stress and temperature. For ambient conditions, a stress-related strain (ε_f) of 0.0035 defines the ultimate compressive strain (ε_{cu}) at failure (CSA A23.3, 2014). For elevated temperatures, El-Fitiany (2013) found it reasonable to predict the ultimate compressive strain (ε_{cuT}) at a value of 0.0035 + ε_{tr}. Free-thermal strains define the expansion of RC materials when exposed to elevated temperatures. Simple equations to determine ε_{th} of siliceous and calcareous aggregate are presented in Eq. 29 and Eq. 30 in Youssef and Moftah (2007). For steel, the ε_{th} can be determined using the reinforcement temperature and the steel coefficient of thermal expansion (α_s). In this paper, the value for α_s was taken from Lie (1992). Transient strain develops during first heating of the concrete. To account for ε_{tr}, a model developed by Terro (1998) is presented in Eq. 35 of Youssef and Moftah (2007). At the point of failure, Terro's equation can be simplified by taking the ratio of current to maximum concrete stress (f_c / f'_c) equal to 1.0.

Three material models are needed in the proposed simplified analysis: concrete compressive strength at elevated temperature (f'_{cT}), steel yield strength at elevated temperature (F_{yT}), and the steel stress-strain relationship at elevated temperature (F_{sT}). The first two models can be represented by Hertz (2005) and Lie (1992). They are found as Eq. 10 and Eq. 38 in Youssef and Moftah (2007). The third model is provided below in Eq. 3 by Lie (1992); T is the steel temperature (°C), ε_{sT} is the steel total strain, and ε_p is the ambient yield strength (F_y in MPa) over 25 x10^4.

[3a] $$F_{sT} = \frac{f(T, 0.001)}{0.001}\varepsilon_{sT} \qquad \varepsilon_{sT} \le \varepsilon_p$$

[3b] $$F_{sT} = \frac{f(T, 0.001)}{0.001}\varepsilon_p + f\left[T, \left(\varepsilon_s - \varepsilon_p + 0.001\right)\right] - f(T, 0.001) \qquad \varepsilon_{sT} > \varepsilon_p$$

[3c] $$where\ f(T, \lambda) = (50 - 0.04T) \times \left[1 - \left(\mathrm{e}^{-30+0.03T}\sqrt{\lambda}\ \right)\right] \times 6.9$$

2.4 Sectional Flexure Analysis

At ambient temperatures, flexural equilibrium conditions can be easily satisfied using the equivalent stress-block parameters (α_1 and β_1). This concept can also be applied to RC beams at elevated temperatures. El-Fitiany and Youssef (2011) proposed Eq. 4 and Eq. 5 to calculate α_{1T} and β_{1T} for sagging and hogging conditions. In Eq. 4 and Eq. 5: p is the reinforcement ratio, f'_c is the ambient concrete strength (MPa), and F_{agg} is a factor to account for aggregate type wherein siliceous aggregate should be taken as zero and calcareous aggregate should be taken as 1.0.

[4a] $$\alpha_{1T} = \alpha_1 - 1.533 \times 10^{-2} + 24.397 \times 10^{-3} t_e + 15.758 \times 10^{-4} f'_c - 10.089 \times 10^{-5} b_c$$

[4b] $$\beta_{1T} = \beta_1 - 2.907 \times 10^{-2} + 20.734 \times 10^{-3} t_e^2 - 94.794 \times 10^{-3} t_e - 75.057 \times 10^{-5} f'_c + 15.413 \times 10^{-5} b_c$$

[5a] $$\alpha_{1T} = \alpha_1 - 2.735 \times 10^{-2} - 1.497 \times 10^{-1} t_e + 7.579 \times 10^{-2} F_{agg}$$

[5b] $$\beta_{1T} = \beta_1 - 1.965 \times 10^{-1} - 4.054 \times 10^{-2} \left(\frac{t_e}{\rho}\right)^2 + 2.448 \times 10^{-1} \left(\frac{t_e}{\rho}\right) - 3.456 \times 10^{-2} F_{agg} + 3.687 \times 10^{-3} f'_c + 2.342 \times 10^{-4} b_c$$

Eq. 6 displays the equilibrium equations, which are identical in form to the ambient, but substituted with the material stresses and stress-block parameters at elevated temperature. Moment capacity at elevated temperature can likewise be solved for by resolving the moment induced by the internal forces (Eq. 7).

[6a] $C_{cT} = \alpha_{1T} \times f'_{cT} \times \beta_{1T} \times c \times b_c$

[6b] $T_{sT} = F_{sT} \times A_s$

[7] $M_{rT} = \sum T_{sT} \left(d - \frac{\beta_{1T} \times c}{2} \right)$

3 CASE STUDY

This section presents an application of the simplified approach for the performance-based flexural fire design of RC beams. The case study is undertaken for a cross-section and natural fire matching the work of Ellingwood and Lin (1991). Their work focused on section internal temperatures during exposure. Failure was not induced during testing, and as such, no ultimate capacity was recorded. To the best of the author's knowledge, no testing has been published recording RC beams tested to capacity failure during exposure to natural fire. Therefore, the results from Ellingwood and Lin (1991) are used to validate the internal temperature approximations, while validation of the flexural capacity is done using ABAQUS FE software.

3.1 Ellingwood and Lin (1991) Beam Parameters

Fig. 1 shows the section details of the experimental beam, measuring 228 x 533 mm in cross-section. Concrete mix design stipulated the use of NSC with Type I Portland cement and calcareous gravel aggregate. Lower longitudinal reinforcement consists of 4-22 mm bars, while upper reinforcement consists of 4-25 mm bars. In the analysis, only lower reinforcement will be considered for the sagging condition, and only upper reinforcement for the hogging condition; therefore, ignoring the effect of compression steel. Shear reinforcement is provided by 10 mm stirrups spaced at 215 mm intervals. Concrete cover is 38 mm. Ambient material properties specified a f'_c of 33.7 MPa and F_y of 420 MPa.

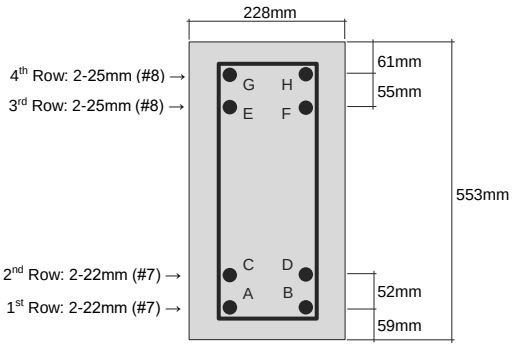

Fig. 1. Ellingwood and Lin (1991) Beam Cross-Section

3.2 Simplified Performance-Based Analysis

Severity of the fire event needs to be represented as a temperature-time relationship. For a compartment fire, this can be achieved using the Eurocode method, but in the case of Ellingwood and Lin (1991), the design fire was experimentally recorded (Fig. 2). The key points for the AITP time equivalent method are identified on the figure as: T_{max} = 1011°C, t_{max} = 37 min, and t_{final} = 145 min. The final duration (t_{final}) is found by linearly extending the cooling branch, ignoring the long extinction period. Using Eq. 1a, the AITP t_e is found to be 96 min, or 1.6 hr. The width of the section is less than 300 mm, and therefore the size adjustment factor is applied at a value of 1.0.

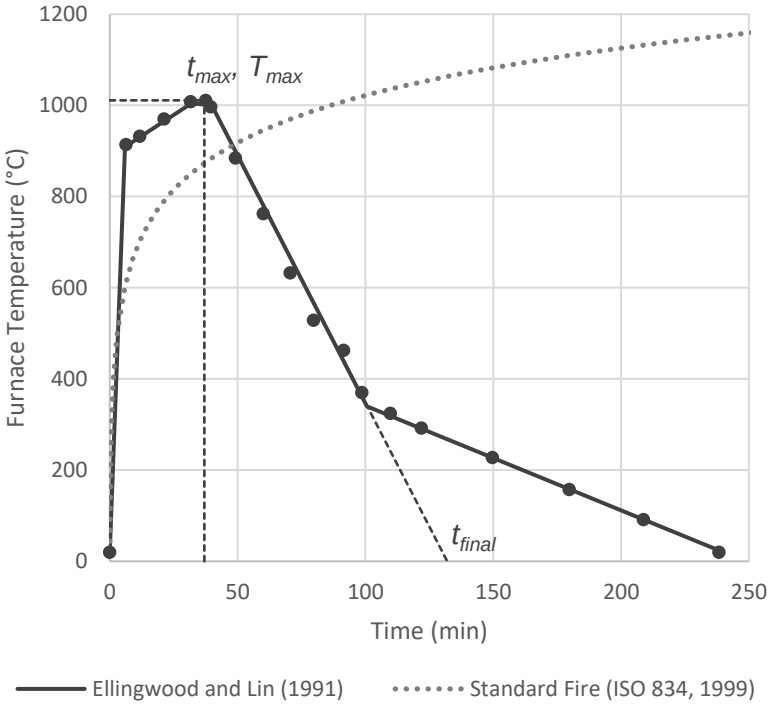

Figure 2. Ellingwood and Lin (1991) Applied Design Fire

Section internal temperatures are calculated using Eq. 2. Considering the selected NSC with calcareous aggregate, the values for the concrete thermal properties are taken as: k = 1.0 $Wm^{-1}K^{-1}$, p = 2400 kgm^{-3}, c_s = 1000 $Jkg^{-1}K^{-1}$, and a_c = 417 x10^{-9} m^2s^{-1} (Lie, 1992). Depending on the mix design and aggregate type, these values can vary greatly between designs.

For the steel bars, temperature is found within the section at the x and y locations of the reinforcement. Because heating is assumed to occur evenly from the two sides, both the left and right bars in a given row exhibit the same temperature. The bar temperatures where found as follows: row 1, 528°C; row 2, 331°C; row 3, 297°C; and row 4, 297°C. Wickström's (1986) method assumes that temperature gradients will become linear at some height, hence rows 3 and 4 recording the same temperature.

Determining the concrete temperature is less straight forward than for the reinforcement, as it varies significantly throughout the section. Material and strain models however require a single input temperature. El-Fitiany and Youssef (2017) have proven that the thermal effects of a fire can be estimated with sufficient accuracy using a concrete average temperature (T_{av}). For the sagging scenario, T_{av} can be found by taking the temperature average along the section's width at a given depth. At the depth of the compression zone, the temperature gradient becomes almost constant with height since heat flow in that region is governed by the two vertical sides. Therefore, by taking the T_{av} within the compression zone, a single concrete temperature can be identified. Using Eq. 2, T_{av} was calculated by sampling internal temperatures along the section's width at a constant height. Samples were taken at 12 width increments and a height of $0.8h_c$. The selected height represents a location where the thermal distribution is assumed to be constant. Taking a weighted average of the samples leads to a value for T_{av} of 412°C for sagging design.

For the hogging condition, temperature gradients at the bottom face vary greatly and do not exhibit the same constant profile experienced near the upper face. As such, calculation of a single T_{av} can not be achieved for a simplified analysis. The resulting equilibrium calculation for hogging is entirely based on steel temperature and does not require a concrete temperature. The effect of non-linear concrete temperature is implicitly included in the stress-block parameters.

Flexural analysis is laid out for the sagging load in Tables 1 and 2. For simplicity, the tension capacity of concrete and compression reinforcement are omitted. Material properties and fire induced strains are first calculated for the concrete section based on T_{av}. Assuming a depth for the neutral axis (c) as 102.2 mm, the force in the compression block is found as 441 kN. Based on a linear strain distribution, Eq. 8 provides the geometric relationship needed to interpolate the concrete strain at the height of the reinforcing rows. Fire induced strains and steel stresses at elevated temperatures are likewise calculated for each layer of steel reinforcement. The c value is iterated until equilibrium between the concrete and steel occurs.

[8] $$\varepsilon_{tots} = \frac{d}{c}\varepsilon_{cuT} - \varepsilon_{totc}$$

Hogging analysis is presented in Table 3. Because a T_{av} could not be determined, concrete strains, and subsequently steel strains, are ignored. Steel yield stress is used in place to the find the tension force at each row of reinforcement. The assumed c value is iterated until equilibrium is satisfied at 146.2 mm. For both sagging and hogging scenarios, Eq.7 finds the maximum sagging and hogging M_{rT} as 178.5 kNm and 257.6 kNm, respectively.

Table 1. Sagging Flexure Analysis for Concrete

(1)	(2)	(3)	(4)	(5)	(6)	(7)	(8)	(9)	(10)
T_{av}	f'_{cT}	α_{1T}	β_{1T}	ε_{tr}	ε_{cuT}	ε_{th}	ε_{totc}	c	C_c
(Eq.2)	(Eq.10)[1]	(Eq.4a)	(Eq.4b)	(Eq.35)[1]	(5)+0.0035	(Eq.30)[1]	(6)-(7)	assume	(Eq.6a)
°C	*MPa*	---	---	*x 10 -3*	*x 10 -3*	*x 10 -3*	*x 10 -3*	*mm*	*kN*
412	33.7	0.85	0.77	11.11	14.61	3.33	11.28	102.2	441

Table 2. Sagging Flexure Analysis for Steel

(1)	(2)	(3)	(4)	(5)	(6)	(7)	(8)	(9)
ID	T	A_s	α_s	ε_{tots}	ε_{th}	ε_{sT}	F_{sT}	T_s
---	(Eq.2)	---	---	(Eq.8)	(2)x(4)	(5)-(6)	(Eq. 3)	(3)x(8)
---	*°C*	*mm²*	*x 10 -5*	*x 10 -3*	*x 10 -3*	*x 10 -3*	*MPa*	*kN*
A, B	528	387	1.41	56.49	7.45	49.04	239	93
C, D	331	387	1.33	49.05	4.42	44.64	331	128

Table 3. Hogging Flexure Analysis for Concrete and Steel

(1)	(2)	(3)	(4)
α_{1T}	β_{1T}	c	C_c
(Eq.5a)	(Eq.5b)	assume	(Eq.6a)[2]
---	*---*	*mm*	*kN*
0.61	1.02	146.2	696

(1)	(2)	(3)	(4)	(5)
ID	T	A_s	F_{yT}	T_s
---	(Eq.2)	---	(Eq. 38)[1]	(3)x(4)
---	*°C*	*mm²*	*MPa*	*kN*
E, F, G, H	297	509	342	174

[1] Equations are referenced to Youssef and Moftah (2007)
[2] In lieu of f'_{cT}, f'_c for ambient temperatures should be used during hogging analysis

3.3 Finite Element Modelling

An ABAQUS model is used to validate the flexural capacity and compliment the experimental temperature results from Ellingwood and Lin (1991). The beam was modelled using solid elements to facilitate the heat transfer analysis, which is not possible using the wire reinforcement approach. To ensure flexural failure, the section outlined in Fig. 1 was given a length of 6 m. Simple support conditions were specified at the ends. Heat transfer was applied based on the given design fire with material properties specified for NSC calcareous aggregate by Lie (1992). Evaluating the fire event as an uncoupled load, the heat transfer profile of the beam was input into the strength analysis as a predefined condition. Uniform loading was applied at various intervals until failure was observed based on strain non-convergence in ABAQUS.

3.4 Comparison with Experimental and Computational Findings

Comparing the simplified analysis with the experimental and ABAQUS results demonstrates the accuracy of the proposed methodology. Fig. 3 presents the internal temperatures for the section based on natural fire (Fig. 3a) and time equivalent fire exposure (Fig. 3b). The general isotherm profiles were developed using ABAQUS. Labelled reinforcement temperatures are based on Ellingwood and Lin's (1991) experimental results for the natural fire (Fig. 3a) and based on Wickström's (1986) method for the time equivalent fire (Fig. 3b).

The time equivalent records moderately conservative temperatures at just about every location within the section. The only exception occurs in the lower middle region, where the time equivalent results in a maximum negative differential of 56°C. This formation is due to the natural fire, with its long duration, being able to slowly heat the internals of the section. The time equivalent fire is not able to match this slow heating effect, and therefore small deviations will generally arise in the lower middle region. Wickström's method found the reinforcement temperatures with a reasonable degree of accuracy. The largest error from the experimental results occurred in row 1 at 32 %. Despite the high error, the simplified analysis resulted in a conservative temperature estimate for the reinforcement. Using the natural fire profile from ABAQUS, calculation of T_{av} at a height of $0.8h_c$ yields 325°C; the simplified analysis at 412°C is 27 % conservative to the ABAQUS result.

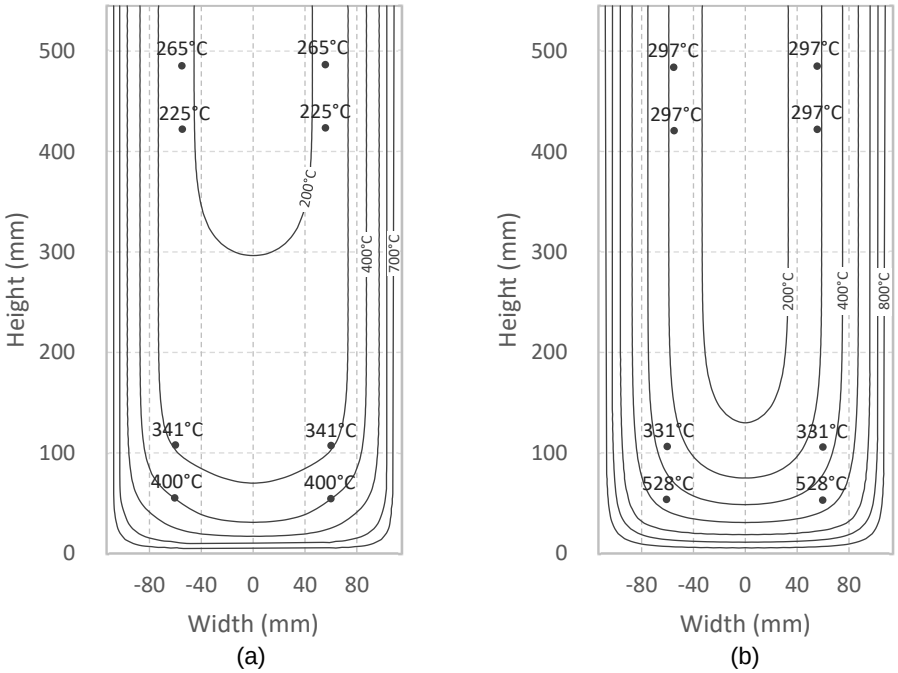

Fig. 3. Thermal Gradients due to (a) Natural Fire and (b) Time Equivalent Fire Exposure

Maximum moment capacity was found by ABAQUS during natural fire exposure to be 198 kNm for the sagging scenario. The simplified analysis resulted in a M_{rT} of 178.5 kNm, incurring a 10 % difference from the FE model. Similarly for the hogging scenario, ABAQUS found the M_{rT} as 284 kNm, 9 % greater than the simplified calculation at 257.6 kNm. In both cases, the simplified analysis resulted in a capacity that was lower, and thus conservative to the FE model.

At ambient temperatures, standard sectional analysis finds the sagging capacity of the section to be 263 kNm and the hogging capacity as 328 kNm. In comparison with the moment capacities of the fire exposed section found by ABAQUS, this represents a 27 % and 14 % capacity reduction for the sagging and hogging conditions, respectively. The marked change in moment capacity from ambient to fire exposed, strongly demonstrates the impact of fire events on RC beams and the necessity of undertaking a simplified analysis as proposed here.

4 CONCLUSIONS

RC structures are used extensively in Canada for high-density and large-scale developments. To facilitate safe evacuation and general occupant safety, designers need to eliminate the possibility of structural collapse during fire events. Performance-based fire design provides a means to determine structural capacity by accounting for fire-induced degradation and stresses. This paper presented the methodology for the simplified flexural analysis of RC beams during fire exposure. For a given compartment, fire severity is determined as a temperature-time relationship and related using a time equivalent to the standard fire. In leu of complex computational programs, a simple thermal model is used to determine the internal temperature at critical locations within the exposed RC element. Substituting material and strain models for RC at elevated temperatures, the equilibrium condition is resolved using the equivalent-stress block method. A case study was provided based on experimental testing to demonstrate the simplified approach. Internal temperatures and flexural capacity were found to be in good agreement with validation based on experimental and computational analysis. The proposed simplified approach enables engineers to design the flexural capacity of RC beams to withstand natural fire events.

5 ACKNOWLEDGEMENTS

The authors are grateful for the support provided by the National Science and Engineering Research Council of Canada (NSERC), the India-Canada Center for Innovative Multidisciplinary Partnerships to Accelerate Community Transformation and Sustainability (IC-IMPACTS), and Western University.

6 REFERENCES

Buchanan, A.H. 2001. *Structural Design for Fire Safety*. 2nd ed., Elsevier, Oxford, UK.

CSA 23.3. 2014. *Design of Concrete Structures*. Canadian Standards Association, Toronto, CA.

Dai, X., Welch, S., and Usmani, A. 2017. A Critical Review of Travelling Fire Scenarios for Performance-Based Structural Engineering. *Fire Safety Journal*, **91**(1): 568-578.

El-Fitiany, S.F. 2013. Simplified Tools for Performance-Based Design of Reinforced Concrete Frames Exposed to Fire. Ph.D. diss, University of Western Ontario.

El-Fitiany, S.F. and Youssef, M.A. 2009. Assessing the Flexural and Axial Behaviour of Reinforced Concrete Members at Elevated Temperatures Using Sectional Analysis. *Fire Safety Journal*, **44**(5): 691-703.

El-Fitiany, S.F. and Youssef, M.A. 2011. Stress-Block Parameters for Reinforced Concrete Beams during Fire Events." *ACI Special Publication: Innovations in Fire Design of concrete Structures*, **SP-279**: 1-40.

El-Fitiany, S.F. and Youssef, M.A. 2017. Fire Performance of Reinforced Concrete Frames Using Sectional Analysis. *Engineering Structures*, **142**(1): 165-181.

Ellingwood, B. and Lin, T.D. 1991. Flexure and Shear Behaviour of Concrete Beams During Fires. *Journal of Structural Engineering*, **117**(2): 440-458.

EN-1991-1-2. 2002. *Eurocode 1: Actions on Structures - Part 1-2: Actions on Structures Exposed to Fire*. European Committee for Standardization, Brussels, BY.

Hertz, K.D. 2005. Concrete Strength for Fire Safety Design. *Magazine of Concrete Research*, **57**(8): 445-453.

Kuehnen, R.T. 2019. Performance-Based Design of Fire-Exposed Reinforced Concrete Elements using an Equivalent Standard Fire. M.E.Sc. thesis, Western University.

Lie, T.T. 1992. *Structural Fire Protection*, ASCE, New York, NY, USA.

NBC. 2015. *National Building Code of Canada*. National Research Council of Canada, Ottawa, CA.

NFC. 2015. *National Fire Code of Canada*. National Research Council of Canada, Ottawa, CA.

Solly, M. 2018. Five Things We've Learned Since Brazil's Devastating National Museum Fire. *Smithsonian Magazine*. www.smithsonianmag.com (accessed Jan 13, 2019).

Terro, M.J. 1998. Numerical Modeling of the Behaviour of concrete Structures. *ACI Structural Journal*, **95-S18**: pp. 183-192.

Wickström, U. 1986. A Very Simple Method for Estimating Temperature in Fire Exposed Concrete Structures. Swedish National Testing Institute *Technical Bulletin*, SP-RAPP 1986(46): 2618-2634.

Youssef, M.A. and Moftah, M. 2007. General Stress-Strain Relationship for Concrete at Elevated Temperatures. *Engineering Structures*, **29**(10): 2618-2634.

ISO 834. 2014. *Fire Resistance Tests – Elements of Building Construction*. International Organization for Standards, Geneva, CH.